

Syracuse University

**SURFACE**

---

Theses - ALL

---

May 2019

## Controlled Synthesis of Pt-Sn/Al<sub>2</sub>O<sub>3</sub> Catalysts and Their Application in the Hydrodeoxygenation of Bio-Based Succinic Acid

Patrick Michael Howe  
*Syracuse University*

Follow this and additional works at: <https://surface.syr.edu/thesis>



Part of the [Engineering Commons](#)

---

### Recommended Citation

Howe, Patrick Michael, "Controlled Synthesis of Pt-Sn/Al<sub>2</sub>O<sub>3</sub> Catalysts and Their Application in the Hydrodeoxygenation of Bio-Based Succinic Acid" (2019). *Theses - ALL*. 329.  
<https://surface.syr.edu/thesis/329>

This Thesis is brought to you for free and open access by SURFACE. It has been accepted for inclusion in Theses - ALL by an authorized administrator of SURFACE. For more information, please contact [surface@syr.edu](mailto:surface@syr.edu).

## Abstract

As environmental and economic forces push for movement away from traditional petroleum-sourced chemical and fuel production, it becomes essential for technologies in renewable carbon resources to be developed. In particular, the production of chemical commodities from renewable lignocellulosic biomass provides a unique path away from the use of petrol. Considering the high density of functional groups present in biomass feedstocks, new technologies must be developed to selectively target the removal of functional groups through the application of supported metal catalysts. The ability to target specific functional group removal would allow for biomass feedstocks to produce higher yields of desired commodities without the production of undesired, lower value chemicals. Through the use of promoter metals, such as Sn, it is possible to shift the selectivities of noble metal catalysts (e.g. Pt, Ru, Pd, etc.), often without greatly reducing the intrinsic activity of the monometallic catalyst. While the usefulness of bimetallic catalysts has been observed in many applications, the actual mechanisms by which promoter metals alter the catalyst's performance is largely left unknown. This gap in knowledge is largely due to the fact that the traditional methods of catalyst synthesis lack the ability to control exact compositions and geometries of surface metal complexes. The synthesis method of strong electrostatic adsorption (SEA) utilizes the surface charging properties of metal oxides to selectively adsorb promoter metals to primary metal sites, potentially allowing for greater control of the composition of metal complexes. This work employs the SEA technique to develop a realistic method for the synthesis of Pt-Sn/Al<sub>2</sub>O<sub>3</sub> bimetallic catalysts. The addition of Sn had profound effects on the selectivity of propionic acid hydrodeoxygenation (HDO), an analog for succinic acid HDO, suppressing nearly all unwanted byproduct production. Through the use of temperature programmed reductions (TPR), ambient-pressure photoemission

spectroscopy (AP-PES), chemical and physical adsorptions, and electron microprobe characterization techniques, this work shows that the changes in propionic acid HDO is likely attributed to the changes in oxidation states of Pt metal sites upon the addition of Sn.

CONTROLLED SYNTHESIS OF PT-SN/AL<sub>2</sub>O<sub>3</sub> CATALYSTS AND THEIR APPLICATION IN THE  
HYDRODEOXYGENATION OF BIO-BASED SUCCINIC ACID

By

Patrick Michael Howe

B.S., SUNY Stony Brook, 2013

Thesis

Submitted in partial fulfillment of the requirements for the degree of  
Master of Science in Chemical Engineering

Syracuse University  
May 2019

Copyright © Patrick Michael Howe 2019

All Rights Reserved

## **Acknowledgements**

Thank you to my advisor, Dr. Jesse Bond, for his guidance and patience over the past 2 years. Dr. Bond's passion for teaching and research is unparalleled and has helped me to become a better student and researcher. Special thanks to Dr. Ben Akih-Kumgeh for agreeing to chair my defense and to Dr. Ian Hosein and Dr. Shikha Nangia for agreeing to be on my defense committee.

Thank you to all past and current members of the Bond Group for their comradery and support, the lab is never short on laughter. Special thanks to Josh Gopeesingh for the countless hours of brainstorming new experiments and data interpretation, but most importantly for being a great friend. Another special thank you to Ran Zhu for his help with the temperature programmed reduction experiments presented in this work.

Thank you to Mario Montesdeoca for his patience and guidance when teaching me to use the atomic absorption spectrometer and for his commitment to educating students on the finer points of analytical chemistry. Thank you to Sally Prash for repairing numerous glass cells broken by clumsy graduate students, as well as her upbeat spirit. Thank you to Dr. Ashley Head of the Center for Functional Nanomaterials at Brookhaven National Laboratory for her help with the photoemission spectrometry experiments presented in this work. Thank you to Dr. Jay Thomas for his help with the electron microprobe experiments presented in this work. Thank you to the faculty and staff of the Biomedical and Chemical Engineering Department, especially Sabina Redington, Jason Markle, and Amy Forbes.

Last, but certainly not least, thank you to my wife, Laura, parents, brother, and friends for their love and support. Graduate school would have been impossible without you.

## Table of Contents

|   |      |
|---|------|
| Abstract .....                                  | i    |
| Acknowledgements.....                           | iv   |
| List of Illustrative Materials.....             | viii |
| Figures .....                                   | viii |
| Tables .....                                    | viii |
| Chapter 1. Literature Review .....              | 1    |
| 1.1 Biofuels and Biochemicals.....              | 1    |
| 1.2 Succinic Acid and Propionic Acid .....      | 2    |
| 1.3 Monometallic and Bimetallic Catalysts ..... | 3    |
| 1.4 Strong Electrostatic Adsorption .....       | 4    |
| Chapter 2. Platinum Adsorption .....            | 6    |
| 2.1 Materials and Methods .....                 | 6    |
| 2.1.1 Catalyst Synthesis.....                   | 6    |
| 2.1.2 Physical Adsorption.....                  | 7    |
| 2.1.3 Chemical Adsorption.....                  | 7    |
| 2.1.4 Metal Loadings by AAS.....                | 9    |
| 2.2 Results and Discussion.....                 | 9    |
| Support Selection.....                          | 9    |
| Differential SEA.....                           | 11   |
| 2.3 Conclusion.....                             | 12   |
| Chapter 3. Tin Adsorption .....                 | 13   |

|   |    |
|---|----|
| 3.1 Materials and Methods .....                         | 13 |
| 3.1.1 Catalyst Synthesis.....                           | 13 |
| Strong Electrostatic Adsorption.....                    | 13 |
| Incipient Wetness Impregnation .....                    | 13 |
| 3.1.2 Chemical Adsorption.....                          | 14 |
| 3.1.3 Metal Loadings by ICP-MS.....                     | 15 |
| 3.1.4 Electron Microprobe.....                          | 16 |
| 3.1.5 Ambient Pressure Photoemission Spectroscopy ..... | 16 |
| 3.1.7 Temperature Programmed Reductions .....           | 17 |
| 3.1.8 Reactor Performance .....                         | 17 |
| 3.2 Results and Discussion.....                         | 20 |
| 3.2.1 Tin Adsorption and Relation to pH .....           | 20 |
| Platinum Leaching .....                                 | 20 |
| Sn Uptake and Chemical Adsorption.....                  | 21 |
| Electron Microprobe X-ray Mapping .....                 | 26 |
| 3.2.2 Effects of Tin on Platinum Catalysts.....         | 27 |
| Reactor Performance.....                                | 27 |
| Temperature Programed Reduction (TPR).....              | 29 |
| Ambient Pressure Photoemission Spectroscopy .....       | 31 |
| 3.3 Conclusion.....                                     | 33 |
| Chapter 4. Conclusion.....                              | 34 |



|                       |    |
|-----------------------|----|
| 4.1 Current Work..... | 34 |
| 4.2 Future Work ..... | 34 |
| References.....       | 36 |
| Vita.....             | 39 |

## List of Illustrative Materials

### Figures

|  |    |
|--|----|
| Figure 1: Succinic acid and propionic acid.....  | 2  |
| Figure 2: Proposed reaction network for propionic acid HDO and subsequent reactions.....   | 3  |
| Figure 3: Representation of charge distribution for optimal Sn adsorption on a Pt/Al <sub>2</sub> O <sub>3</sub> base catalyst.....  | 10 |
| Figure 4: Calibration curve for actual sample temperature based on sample temperature reading.....   | 16 |
| Figure 5: Experimental reactor setup.....  | 19 |
| Figure 6: Sn adsorption normalized by the amount of Pt on the base catalyst surface over a range of synthesis pH's. Significant Sn uptake can be seen in the range of pH 1 – 3.....  | 21 |
| Figure 7: Pt L $\alpha$ and Sn L $\alpha$ x-ray mapping of a 2.56%Pt/2.53%Sn bimetallic catalyst. Circled areas indicate regions of possible corresponding Pt and Sn intensities.....  | 27 |
| Figure 8: Changes in selectivity of HDO, methanation, hydrogenolysis, and water-gas shift reactions at 469 K, 5 torr propionic acid, and 755 torr H <sub>2</sub> .....   | 28 |
| Figure 9: TPR profiles of mono and bimetallic catalysts synthesized using IW and SEA methods.....  | 30 |
| Figure 10: a) Al <sub>2</sub> p and Pt <sub>4</sub> f lines of a Pt/Al <sub>2</sub> O <sub>3</sub> catalyst b) Al <sub>2</sub> p and Pt <sub>4</sub> f lines of a fresh Pt-Sn/Al <sub>2</sub> O <sub>3</sub> catalyst c) Al <sub>2</sub> p and Pt <sub>4</sub> f lines of a spent Pt-Sn/Al <sub>2</sub> O <sub>3</sub> catalyst..... | 32 |

### Tables

|  |    |
|--|----|
| Table 1: BET surface areas of three potential Al <sub>2</sub> O <sub>3</sub> supports.....   | 10 |
| Table 2: Comparison of two Al <sub>2</sub> O <sub>3</sub> powdered supports.....   | 11 |
| Table 3: Differential SEA Pt adsorptions.....  | 12 |
| Table 4: Platinum leaching in initial Sn adsorption experiments quantified by AAS.....   | 20 |
| Table 5: Metal loadings of Pt/Al <sub>2</sub> O <sub>3</sub> and Pt-Sn/Al <sub>2</sub> O <sub>3</sub> catalysts. Pt-Sn/Al <sub>2</sub> O <sub>3</sub> catalysts are named for the initial pH of synthesis solution and the percent of Pt recovered from the base catalyst is provided to indicate when leaching has occurred during synthesis..... | 23 |

|   |    |
|---|----|
| Table 6: Chemical adsorptions of CO, H <sub>2</sub> , and O <sub>2</sub> on Pt/Al <sub>2</sub> O <sub>3</sub> base catalysts and Pt-Sn/Al <sub>2</sub> O <sub>3</sub> bimetallic catalysts. Metal dispersion was calculated using CO adsorption data..... | 24 |
| Table 7: Pt/Al <sub>2</sub> O <sub>3</sub> 1 CO adsorption results showing initial drops in metal dispersion with multiple reductions.....  | 26 |
| Table 8: Metal loadings of SEA and IW catalysts used in TPR experiments.....  | 29 |
| Table 9: Metal loadings of SEA catalysts used in AP-PES experiments.....  | 31 |

## **Chapter 1. Literature Review**

### **1.1 Biofuels and Biochemicals**

With growing concerns regarding the environmental, political, and societal impacts of chemicals and fuels produced from petrol, it is essential that new sources of these commodities be developed[1,2]. The factors necessitating the development of new sources include the rising prices of crude oil, the effects of carbon emissions on the global climate, and the desire for the United States to become energy self-sufficient[1,3]. Historically, the production of many of the chemical building blocks used to produce high value commodities have been the byproducts of ethylene production via naphtha cracking[4]. Due to the abundance of natural gas, ethylene production has shifted from the traditional petrol feedstock and has subsequently diminished the production of the chemical building blocks produced as byproducts[4]. In an effort to both reduce carbon emissions and counter the reduced production of naphtha cracking coproducts, the use of biomass as a chemical feedstock has come to the forefront of research in the chemical industry[2,4].

Biomass is the only available renewable source of fixed carbon for the production of chemical commodities and fuels, but due to the high density of oxygenated functional groups it is difficult to upgrade into useful chemical building blocks[5,6]. Specifically, this functionality makes it difficult to synthesize the liquid alkanes used as fuels because they require the removal of many of the functional groups present in bio-oil[5]. It more likely that biomass feedstocks will be competitive in markets where the functional groups of bio-oil are an advantage over petrol feedstocks that require the addition of these groups[5]. The development of technologies that will allow for the targeted removal of specific functional groups is essential to the competitiveness of biomass-derived chemical feedstocks.

## 1.2 Succinic Acid and Propionic Acid

In 2004, the United States Department of Energy named succinic acid (Figure 1) as one of the 12 potential building blocks for synthesizing chemical commodities from biomass[7]. Succinic acid is a C<sub>4</sub>-diacid containing two carboxylic acid functional groups[4]. Succinic acid is synthesized from lignocellulosic biomass through microbial fermentation and recovered from the fermentation broth through methods of membrane separation, chromatography, direct crystallization, and precipitation[8,9]. This building block is of particular interest due to use in the synthesis of a variety of commodities, such as coatings, surfactants, green solvents, and biodegradable plastics[8,10]. Some notable upgraded products of succinic acid include, 1,4-butanediol, tetrahydrofuran, and gamma-butyrolactone, which are acquired through

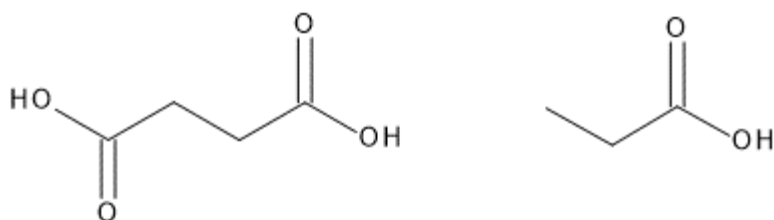


**Figure 1:** Succinic acid (left) and propionic acid (right)

hydrodeoxygenation reactions. [9,10]. HDO is the removal of oxygen containing functional groups through hydrogenolysis and is the pathway utilized to produce higher value commodities from succinic acid[4]. Due to the high activity of noble metal catalysts used in HDO reactions, there are several undesired side reactions that occur, such as decarboxylation and decarbonylation, leading to decreased yields of targeted products. This motivates a deeper study of succinic acid HDO and how tuning catalysts with secondary promoter metals might increase the yield of upgraded commodities.

To understand the mechanisms of catalytic hydrodeoxygenation (HDO) reactions, propionic acid (Figure 1) was selected as an analog to succinic acid. Like succinic acid,

propionic acid contains a carboxylic acid functional group, but has a lower boiling point and is therefore more easily vaporized for gas phase reactions conducted in packed bed reactors (PBR).

The proposed network for propionic acid HDO and subsequent reactions is shown in Figure 2.

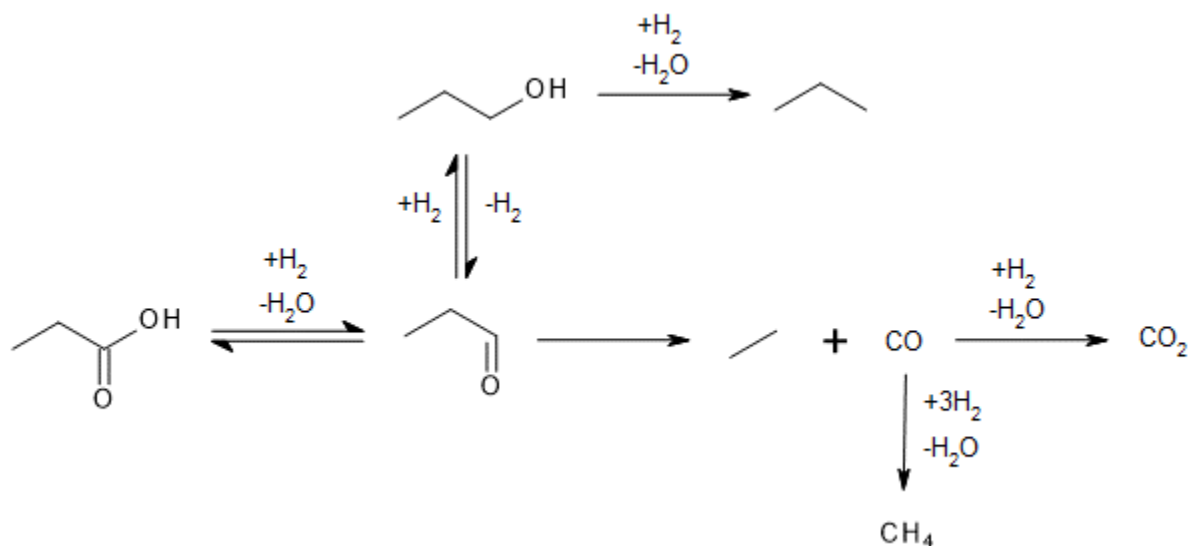


**Figure 2:** Proposed reaction network for propionic acid HDO and subsequent reactions

### 1.3 Monometallic and Bimetallic Catalysts

Due to the high number of functional groups present in lignocellulosic biomass feedstocks it can be difficult to target specific products with traditional monometallic catalysts[2]. To improve catalyst performance in these applications, it is useful to apply the concept of bimetallic catalysts, where a promoter metal is added to the primary active metal to affect catalyst stability, selectivity, and catalytic activity[2,11].

One category of secondary metals that is of interest is the oxophilic promoter. An oxophilic metal, such as Sn, may perturb the electronic or physical environment of the primary metal by remaining partially oxidized under reaction conditions[12]. Bimetallics are most commonly synthesized through either incipient wetness sequential impregnation and co-impregnation[13–15]. The issue with this synthesis method lies within the methods inability to

control the placement secondary metals to ensure the homogeneity of active sites[13]. Often, the surface will be covered in monometallic and bimetallic clusters that have migrated to their thermodynamically stable formations and have large average sizes that reduce the amount of active metal available for reaction[13,14]. Gaining a deeper understanding of kinetic information from these different surface sites can prove to be not only challenging, but often impossible. Changes may be able to be inferred based on the addition of a secondary metal, but the true reaction rates, barriers, and other kinetic properties cannot be parsed from the mix of active site available[2,14]. In order to understand the chemical and physical changes that allow these changes in reaction kinetics, one must target the controlled synthesis of bimetallic active sites through a method that allows for the selective deposition of secondary metals.

#### **1.4 Strong Electrostatic Adsorption**

Strong electrostatic adsorption (SEA) is a proven method for monometallic and bimetallic supported catalysts that leverages the charging properties of oxides when placed in solution[13,15]. The oxide supports, such as alumina and silica, will have a net charge, centered around the point of zero charge (PZC), based on the pH of solution they are placed in. The PZC is the pH at which a support oxide will have a net zero charge over its surface and is a property that varies with the chosen support. By raising the pH above the PZC, one can deprotonate the surface hydroxyls creating a net negative support charge with the opposite being true for solution pH's below the PZC. This ability to leverage surface charge allows for the selection of cationic and anionic metal complexes that will be adsorbed to the support surface. For example, a platinum anion complex in solution, such as hexachloroplatinate, will adsorb to the surface of silica or alumina if the pH of solution is below the PZC of the support oxide[15]. This is due to

the protonation of the support's surface oxides, creating a net positive charge that drives the anions to adsorb to the surface[15].

The SEA method has been proven to produce highly dispersed metal nanoparticles that have a much narrower size distribution than traditional methods of catalyst synthesis[11]. Current research has shown that the application of SEA extends past the synthesis of monometallic catalysts and has the potential to create bimetallics through selective adsorption[11,13,15]. By selecting supports and primary metals that have different PZC's, it is possible to manipulate the pH of synthesis solution and produce a surface where the primary metal and support oxides have opposite charges. This difference in surface charge would create the potential for selective secondary metal ion adsorption to the primary metal oxides through a set of sequential SEA syntheses[15]. The method by which to synthesize these bimetallics is varied and can have effects on the structure of nanoparticles (e.g. core-shell and mixed alloy structures)[15]. As discussed in the previous section, the potential to selectively adsorb secondary promoter metals is appealing to those who want to study reaction kinetics because it would ensure that active sites are homogeneous in their metal composition.

The motivation for this project is to develop a method for the controlled synthesis of supported Pt-Sn catalysts to generate a suite of materials that will be tested to determine their ability to tune the selectivity of propionic acid hydrodeoxygenation (HDO). It is our hypothesis that the SEA method can be used to produce these catalysts and that through characterization and probe reactions, we will gain a deeper understanding of how oxophilic promoters change the performance of noble metal catalysts under practical reaction conditions.



## Chapter 2. Platinum Adsorption

### 2.1 Materials and Methods

#### 2.1.1 Catalyst Synthesis

Platinum supported catalysts were synthesized via the method of strong electrostatic adsorption (SEA). Alumina supports were sourced from Strem Chemicals and Inframat Advanced Materials in powdered and pellet forms with a minimum 97% purity and were sieved to select for 45 to 90 micron sized particles. All supports were prepared for synthesis by calcination under flowing air (Airgas, Ultra Zero Air) at a minimum of 50 mL/min for 3 hours at 623 K with a 3 K/min ramping. Hydrogen hexachloroplatinate(IV) hydrate (Acros Organics) was used as a metal precursor for the synthesis of catalysts on alumina supports and synthesis solutions were made to have a Pt concentration of 200  $\mu\text{g/mL}$  in deionized water. An initial pH measurement was taken using a Milwaukee MW 102 pH/Temp Meter with a SE220 probe. The meter was calibrated using pH 4.01 and pH 7.01 (Milwaukee) buffer solutions prior to every synthesis. The pH of synthesis solutions was adjusted to the target starting conditions using hydrochloric acid (Fisher Scientific, Trace Metal Grade) solutions. Synthesis solutions were poured over supports and placed on an orbital shaker for 1 hour at 80 rpm. The synthesized catalysts were then filtered from solution and dried in an oven at 373 K for a minimum of 12 hours. Catalysts were then calcined in air at 623 K for 3 hours and subsequently reduced in hydrogen (Airgas, Ultra High Purity) at 673 K for 4 hours. After reduction, catalysts were passivated by flowing a 1%Ar/1%O<sub>2</sub>/98%He blend (Airgas) for a minimum of 15 minutes. All temperature ramps were 3 K/min with minimum gas flows of 50 mL/min.

### 2.1.2 Physical Adsorption

A Micromeritics ASAP 2020 system was used to perform physical adsorption experiments on alumina supports to estimate the available surface area for metal precursors to adsorb on during catalyst synthesis. Samples of 100 – 200 mg were loaded into a Micromeritics quartz physisorption analysis cell with an initial sample mass measured on a Denver Instrument TP-214 analytical balance. Samples are degassed on the Micromeritics ASAP 2020 by initially evacuating the sample to a vacuum setpoint of 500  $\mu\text{mHg}$  while increasing the temperature to 363 K at a ramp rate of 3 K/min and holding for 1 hour. After the initial evacuation phase the sample temperature was ramped to 523 K at 3 K/min and evacuated for 4 hours, then cooled and backfilled with gaseous  $\text{N}_2$  (Airgas, Ultra High Purity). After degassing, the samples were reweighed, and a more accurate sample mass was obtained due to the removal of adsorbed water from atmospheric exposure.

To obtain the Brunauer-Emmett-Teller (BET) surface area, samples were lowered into a liquid  $\text{N}_2$  (Airgas) bath and evacuated to a setpoint of 10  $\mu\text{mHg}$  and held for 6 minutes. Samples were then dosed incrementally with gaseous  $\text{N}_2$  from 0 – 1 relative pressure and the BET surface area was obtained from the quantity adsorbed at relative pressures from 0.06 – 0.3. Relative pressure is defined as the pressure of  $\text{N}_2$  dosed divided by the measured vapor pressure of  $\text{N}_2$ .

### 2.1.3 Chemical Adsorption

A Micromeritics ASAP 2020 system was used to perform chemical adsorption experiments on catalysts to estimate the number of Pt surface sites and metal dispersion. Carbon monoxide was used as the analysis gas for all catalysts in this chapter.

#### **Chemisorption Method 1:**

Samples were loaded into a Micromeritics quartz chemisorption analysis cell with an initial sample mass measured on a Denver Instrument TP-214 analytical balance. Samples were degassed on the Micromeritics ASAP 2020 by initially evacuating the sample to a vacuum setpoint of 10  $\mu\text{mHg}$  while increasing the temperature to 363 K at a ramp rate of 3 K/min. After the initial evacuation phase the sample temperature was ramped to 523 K at 3 K/min and evacuated for 2 hours, then cooled and backfilled with gaseous  $\text{N}_2$  (Airgas, Ultra High Purity). After degassing, the samples were reweighed to obtain a dry sample mass.

For analysis, the system was initially evacuated to a vacuum setpoint of 10  $\mu\text{mHg}$  at 308 K for 30 minutes and backfilled with He (Airgas, Ultra High Purity). The sample temperature was then ramped to 383 K at 3 K/min and evacuated for an additional 30 minutes, then cooled to 373 K. The system was evacuated for 30 minutes, then cooled to 308 K and evacuated for an additional 30 minutes. The sample was reduced in pure  $\text{H}_2$  (Airgas, Ultra High Purity) for 2 hours at 673 K. The system was evacuated for 30 minutes, then cooled to 308 K and evacuated for an additional 30 minutes. A leak test was performed to ensure that the outgas rate was below the acceptable limit of 10  $\mu\text{mHg}/\text{min}$ . The system was evacuated for 10 minutes before performing sample analysis. CO analysis was performed at 308 K with data being extrapolated from dosing pressures of 100, 150, 200, 250, 300, 350, 400, 450 mmHg. An initial analysis was performed giving a combined quantity of both chemically and physically adsorbed gas species. A repeat analysis was performed to determine a quantity for only physically adsorbed species after evacuating the sample for 30 minutes. The repeat analysis was then subtracted from the initial analysis, providing the quantity of chemically adsorbed gas species.

### 2.1.4 Metal Loadings by AAS

To obtain metal loadings of Pt/Al<sub>2</sub>O<sub>3</sub> catalysts, synthesis solution concentrations were measured before and after catalyst synthesis by atomic absorption spectroscopy (AAS). Measurements were made on a Perkin Elmer AAnalyst 300 and quality control samples were created with primary and secondary stock solutions from High-Purity Standards and Sigma-Aldrich respectively. Sources were diluted by weight to a curve range from 2 – 200 µg/mL using a 5% HCl and 1% LaCl<sub>3</sub> in HCl solutions. Samples were also diluted using the same solutions to be within the curve range.

## 2.2 Results and Discussion

### Support Selection

For selective electrostatic adsorption of promoter metals onto monometallic supported catalysts, it is vital to select a support whose PZC is distant enough from that of the primary metal on the surface. Having significant separation between the PZC's should ensure that there is some optimal range of pH's where the net charges of the primary metal oxides and support oxides will be opposite when placed in the synthesis solution. In the case of Sn adsorption, Sn cations are available in solution for adsorption to the surface and for the ions to selectively adsorb to platinum oxide (PtOx) species it is essential that the net charge of Pt species is negative while the support charge is positive. Being that the charge of metal oxides is a net charge and not an absolute one, means that if the PZC's of primary metal and support are too close, selective adsorption is likely to be unobtainable. Adsorption of Pt metal complexes has been extensively researched on both alumina and silica, therefore these were considered as support candidates for Pt-Sn bimetallics[13,15,16]. A literature search revealed that the PZC of PtOx species would be at approximately pH of 1 and therefore alumina, which has a PZC of approximately 8.5, was

determined to be a better candidate than silica, which has a PZC of approximately 4[15]. The wider difference in pH between alumina and PtOx should be sufficient enough to produce a range of pH's where selective Sn adsorption can be achieved. Figure 3 is a representation of what the hypothesized charge distributions would be over a Pt/Al<sub>2</sub>O<sub>3</sub> surface for optimal Sn adsorption.

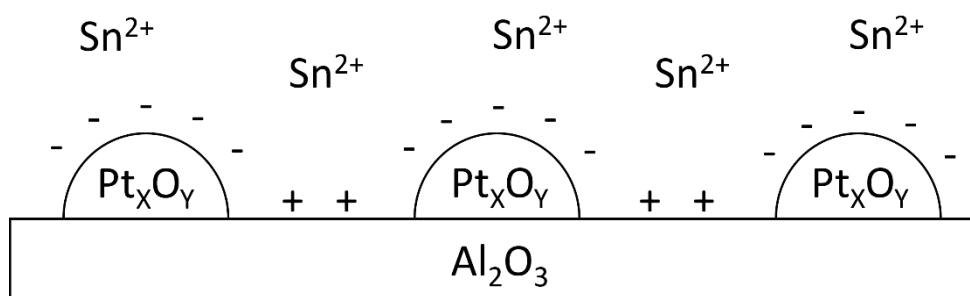


**Figure 3:** Representation of charge distribution for optimal Sn adsorption on a Pt/Al<sub>2</sub>O<sub>3</sub> base catalyst

The available support surface area for metal ion complexes to adsorb to was determined to be of importance. This is due to the fact that if the support surface area is too low, very little metal will adsorb to the surface and the metal loadings of the catalysts will be reduced. This would in turn increase the size of reactor beds required to achieve the targeted conversions for reactor performance studies.

**Table 1:** BET surface areas of three potential Al<sub>2</sub>O<sub>3</sub> supports

| Sample               | BET Surface Area (m <sup>2</sup> /g) |
|----------------------|--------------------------------------|
| Inframat Powder      | 40.0 ± 0.2                           |
| Ground Strem Pellets | 231.3 ± 0.4                          |
| Strem Powder         | 206.5 ± 0.5                          |

Physical adsorption studies were conducted on three alumina supports to determine BET surface area, shown in Table 1. From this data, it is clear that the powder support sourced from

Inframat would have a surface area that was far too low, making it difficult to achieve metal loadings above 0.5%, to be discussed later. Since the surface was comparable to that of the ground pellets, it was concluded that the Strem powder source would be selected due it already being a powdered form, thus limiting the possible contamination of the support powder from grinding pellets in a ceramic mortar and pestle. Metal loadings calculated from AAS confirmed that under similar conditions, the Inframat powder's lower surface area hindered the adsorption of Pt complexes when compared with the Strem powder, as seen in Table 2. Metal loadings are defined as:

$$\text{Metal Loading} = \frac{m_{Pt}}{m_{Pt} + m_{support}} \times 100$$

$$m_{Pt} = (\Delta Conc) \times V_{syn}$$

where  $\Delta Conc$  is the difference of the initial and final concentrations of the synthesis solution,  $V_{syn}$  is the volume of synthesis solution, and  $m_{support}$  is the mass of support used.

**Table 2:** Comparison of two Al<sub>2</sub>O<sub>3</sub> powdered supports

| Support         | Mass of Support (g) | Synthesis pH | Pt Weight (%) |
|-----------------|---------------------|--------------|---------------|
| Inframat Powder | 0.8                 | 2.56         | 0.43          |
| Strem Powder    | 0.5                 | 2.78         | 2.5           |

### Differential SEA

A differential SEA experiment was performed to verify the parameters that control the adsorption of metal precursors to the surface of support oxides. This experiment sought to prove that by controlling the pH of synthesis solution, it is possible to control the adsorption of metal ions regardless of the amount of support provided for synthesis. A minimal amount of support

was placed in solution with an excess amount of Pt precursor to prevent changes in pH throughout the experiment. As an added control, the pH of solution was maintained using diluted hydrochloric acid. The minor changes in Pt concentration during adsorption were beyond the limits of the AAS and therefore results were reliant upon the chemical adsorption of CO. As the results in Table 3 show, the two catalysts yielded comparable CO chemical adsorption results despite the differences in masses provided during synthesis. This confirmed that the driving force of SEA is the pH of the synthesis solution and that when providing an excess of metal precursor ions, reproducible catalyst site counts could be maintained independent of the amount of catalyst being synthesized.

**Table 3:** Differential SEA Pt adsorptions

| Mass of Support (g) | Initial pH | Final pH | CO Uptake ( $\mu\text{mol}/\text{g}_{\text{cat}}$ ) |
|---------------------|------------|----------|---|
| 0.0443              | 2.41       | 2.41     | $91.9 \pm 1.0$                                      |
| 0.0232              | 2.40       | 2.43     | $94.4 \pm 1.4$                                      |

### 2.3 Conclusion

When selecting supports for the synthesis of bimetallic supported catalysts by SEA, it is necessary to choose a support whose PZC properties will provide a range for optimal adsorption to the support that is separate from that of the primary metal oxide. For this reason, alumina was selected over silica as the preferred support for Pt-Sn bimetallic synthesis. The surface area available for metal complex adsorption is essential in increasing loadings when synthesizing Pt/Al<sub>2</sub>O<sub>3</sub> monometallic catalysts. It should also be noted that regardless of the mass of support provided, reproduceable Pt complex adsorption can be achieved when controlling synthesis solution pH, confirming pH to be the driving force of SEA synthesis.

## **Chapter 3. Tin Adsorption**

### **3.1 Materials and Methods**

#### **3.1.1 Catalyst Synthesis**

##### **Strong Electrostatic Adsorption**

Platinum catalysts were synthesized to serve as base catalysts for the synthesis of platinum-tin bimetallic catalysts and followed the same procedure from section 2.1.1. However, after passivation, platinum catalysts were calcined again prior to use in Sn adsorption experiments. This extra calcination was found to be necessary to aid in the prevention of platinum leaching when exposed to Sn synthesis solutions. Tin(II) chloride dihydrate (Acros Organics, 98+%) solutions were prepared in deionized water to a concentration of 300  $\mu\text{g/mL}$  and adjusted to the experimental pH using hydrochloric acid (Fisher Scientific, Trace Metal Grade) and sodium hydroxide (Sigma-Aldrich,  $\geq 98\%$ ) solutions. Sn adsorption experiments were conducted and catalysts were prepared for use in reaction experiments using the same method outlined in section 2.1.1 with the pH meter being calibrated using pH 7.01 (Milwaukee) and 10.01 (Oakton) buffer solutions for experiments conducted in the basic range.

##### **Incipient Wetness Impregnation**

For the purposes of comparing traditional synthesis methods with SEA, mono and bimetallic catalysts were synthesized by incipient wetness impregnation (IW). Aqueous solutions of tin(II) chloride and hydrogen hexachloroplatinate(IV) hydrate were made at varying concentrations based on desired metal loading. The solutions were then added dropwise onto alumina support until incipient volume was reached and then briefly sonicated to ensure complete dispersion of the solution. The catalysts were then allowed to air dry for 12 hours and then placed in a drying oven at 323 K for an additional 12 hours. Catalysts were then calcined in



air at 623 K for 3 hours and subsequently reduced in H<sub>2</sub> at 673 K for 4 hours. After reduction, catalysts were passivated by flowing a 1%Ar/1%O<sub>2</sub>/98%He blend (Airgas) for a minimum of 15 minutes. All temperature ramps were 3 K/min with minimum gas flows of 50 mL/min. Pt-Sn bimetallic catalysts were synthesized by sequential addition of Sn onto prepared Pt/Al<sub>2</sub>O<sub>3</sub> catalysts.

### **3.1.2 Chemical Adsorption**

Chemical adsorption experiments were performed on catalysts to estimate the number of catalytically active sites and metal dispersion. Initially CO chemisorption was used on monometallic Pt catalysts, but as Sn was added to these catalysts it was necessary to acquire H<sub>2</sub> and O<sub>2</sub> chemisorption data. This is due to the fact that Sn is unable to chemically adsorb CO and the changes in H<sub>2</sub> and O<sub>2</sub> may indicate the adsorption of Sn to Pt base catalysts[14]. For this reason, there are two separate methods used in this phase of the project, Method 1 (refer to section 2.1.3) being used during preliminary Sn experiments and Method 2 being a more refined study used to characterize monometallic and bimetallic catalysts synthesized for the Sn adsorption study.

#### **Chemisorption Method 2:**

Loading and degas methods are the same as mentioned for Chemisorption Method 1 referenced in section 2.1.3. The system was initially purged with He at 308 K for 5 minutes and then the temperature was ramped to 373 K at 3 K/min and held for 10 minutes. The system was evacuated for 30 minutes, then cooled to 308 K and evacuated for an additional 30 minutes. All method evacuations were performed by evacuating to a maximum pressure of 5 µmHg. H<sub>2</sub> was flown for 5 minutes and then ramped to 673 K at 3 K/min for 240 minutes to reduce the catalyst. The system was evacuated for 30 minutes, then cooled to 308 K and evacuated for an additional

30 minutes. A leak test was performed to ensure that the outgas rate was below the acceptable limit of 10  $\mu\text{mHg}/\text{min}$ . The system was evacuated for 10 minutes before performing sample analysis. CO, H<sub>2</sub>, and O<sub>2</sub> analyses were performed at 308 K with data being extrapolated from dosing pressures of 100, 150, 200, 250, 300, 350, 400, 450 mmHg. An initial analysis was performed giving a combined quantity of both chemically and physically adsorbed gas species. A repeat analysis was performed to determine a quantity for only physically adsorbed species after evacuating the sample for 60 minutes. The repeat analysis was then subtracted from the initial analysis, providing the quantity of chemically adsorbed gas species.

### **3.1.3 Metal Loadings by ICP-MS**

To acquire metal loadings of Pt and Pt-Sn supported catalysts it was necessary to perform an aqua regia digestion to completely dissolve the sample for analysis by inductively coupled plasma mass spectrometry. Digestions were performed by weighing 25 – 30 mg of catalyst into a round bottom flask and then dissolved in aqua regia. Aqua regia solution was produced by mixing 7 mL of hydrochloric acid (Fisher Scientific, TraceMetal Grade) and 3 mL of nitric acid (Fisher Scientific, TraceMetal Grade) in a graduated cylinder. Digestion was maintained at a uniform 373 K using a mineral oil bath. The reactants were constantly mixed by a teflon stir bar and evaporated solution was condensed in a reflux system cooled to 288 K by a Neslab RTE-111 circulator pumping at 15 L/min. After 12 hours the reactants were rinsed from the round bottom flask using deionized water and diluted to 25 mL in a volumetric flask. Digestions were further diluted by mass in 1% nitric acid for ICP-MS analysis. Pt and Sn primary and secondary sources were obtained from High-Purity Standards and Sigma-Aldrich and diluted by mass using 1% nitric acid (Fisher Scientific, OPTIMA Grade) to a curve range of 10 – 300 ng/mL. Sample

digestions were also diluted by mass in a 1% nitric acid solution to be with the curve range. ICP-MS analysis was conducted on a Perkin Elmer Elan 6100.

### 3.1.4 Electron Microprobe

Electron microprobe experiments were conducted on a Cameca SXFive equipped with a LaB<sub>6</sub> cathode and five wavelength dispersive spectrometers. Powdered catalysts were set in epoxy and then ground flat and polished before being loaded into the instrument. Pt L $\alpha$  and Sn L $\alpha$  x-rays were counted and compiled into a map of metal dispersion on the surface of an individual Pt-Sn/Al<sub>2</sub>O<sub>3</sub> support particle.

### 3.1.5 Ambient Pressure Photoemission Spectroscopy

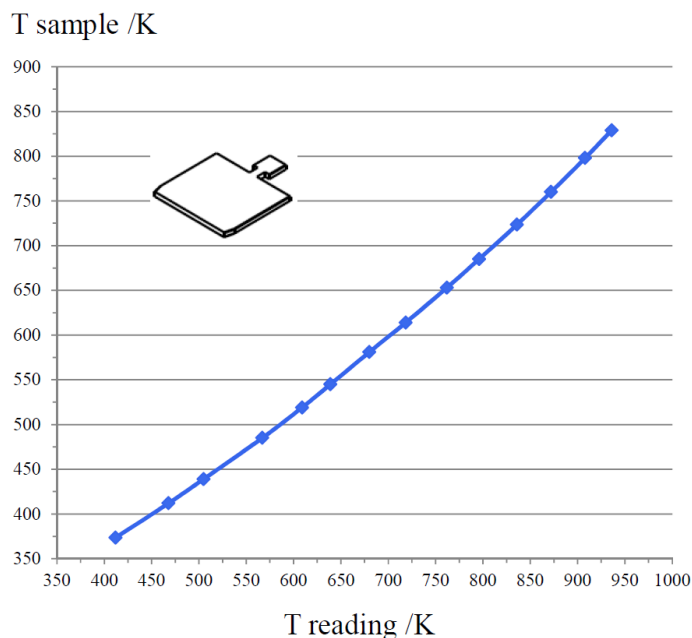


**Figure 4:** Calibration curve for actual sample temperature based on sample temperature reading

Experiments were conducted on an ambient pressure photoemission spectrometer (AP-PES) equipped with a PHOIBOS NAP (near-ambient pressure) analyzer, manufactured by SPECS Surface Nano Analysis GmbH, in collaboration with the Center for Functional

Nanomaterials at Brookhaven National Laboratory. Samples were pressed onto copper plates using minimal force, ensuring the powdered catalyst would remain in place during analysis, and loaded into the analysis chamber at pressure of less than  $5 \times 10^{-9}$  mbar. Analysis was conducted using a monochromated Al K $\alpha$  photon beam, focused to 300  $\mu\text{m}$ , separated from the analysis chamber by an aluminum coated silicon nitride membrane. Photoelectrons were collected through a 300  $\mu\text{m}$  conical aperture and focused with electrostatic lenses before reaching the analyzer. Samples were dosed with 1 mbar of H<sub>2</sub> via precision leak valves. Temperature was controlled using a heating lamp and monitored with a thermocouple in contact with the sample holder. Figure 4 shows the calibration curve, provided by the manufacturer, for actual sample temperature with respect to the temperature reading[17].

### **3.1.7 Temperature Programmed Reductions**

Pt/Al<sub>2</sub>O<sub>3</sub> and Pt-Sn/Al<sub>2</sub>O<sub>3</sub> catalysts were loaded into a quartz cell with the target mass being 200 – 300 mg. Catalyst samples were dried in flowing He (Airgas Ultra High Purity) at a rate of 30 mL/min at 393 K for 120 minutes. Samples were then allowed to cool to 323 K while remaining in He flow. Temperature programmed reductions (TPR) were performed from 323 K to between 1073 K and 1173 K, depending metal composition, at a rate of 10 K/min. TPR samples were exposed to a continuous flow of a 1% Ar/5% H<sub>2</sub>/94% He blend (Airgas) at a rate of 30 mL/min. Partial pressures of gases and hydrogen uptake were measured using an SRS RGA100 residual gas analyzer.

### **3.1.8 Reactor Performance**

Liquid reactants were sent for pretreatment from glass syringes (Hamilton) using a syringe pump (Cole Parmer) via capillary PEEK tubing (McMaster) where it was vaporized and swept to a fully reduced packed bed reactor by H<sub>2</sub>. Gas Feeds were delivered using digital mass

flow controllers (Brooks); the experimental volumetric flow rate was measured using a bubble flow-meter since in some instances, the digital volumetric flow rate on the mass flow controller did not match the actual volumetric flow rate. The temperature of the vaporizer was maintained at conditions in accordance with Antoine Coefficients to ensure that all liquid feeds entered and remained in the gas phase. The vaporizer consisted of stainless-steel furnace that was heated using a band heater (McMaster), which encapsulated a 0.25-inch diameter dead volume that was filled with quartz chips. The dead volume served as a medium where the liquid feed came into contact with the reactant/carrier gas, quartz chips served to ensure dispersion and uniform vaporization. The temperature of the vaporizer furnace was measured using type-K thermocouples (Omega) and power was supplied to the band heater using a temperature controller (Omega). Species flowed through a two-position 6 port valve that directed reactants to the reactor or a bypass leading straight to the gas chromatograph. Before sending reactants to the reactor system, reactant signals were observed in the bypass to be certain the liquid feed was completely vaporized. Bypass signals coupled with the volumetric flow rate from the bubble meter also serves as a final leak test before sending species to the reactor.

The reactor system consisted of a 1/2-inch stainless steel tube (McMaster) that was used as an up-flow packed bed reactor. The reactor consisted of quartz chips to achieve full dispersion across the diameter of the tubing to ensure the entire gaseous species came into maximum contact with the catalyst bed. The bed was sandwiched between quartz wool to keep it intact and prevent catalyst loss. The reactor was placed in a stainless-steel furnace controlled by a band heater. The temperature of the reactor furnace was measured using type-K thermocouples (Omega) and power was supplied to the band heater using a temperature controller (Omega). The temperature was also measured at the catalyst bed to account for the temperature gradient that

exists between the bed and walls of the furnace; this was measured by a type-K thermocouple. Tubing between reactor and the analysis systems was 1/8-inch stainless steel (McMaster) that was heat traced using nichrome wire (McMaster), which was fed power by a variac transformer; the heating of the tubing served the purpose of making sure all chemicals remained in the gas phase for proper analysis. The chemical species were analyzed by gas chromatography (HP5890) using a HP-PONA column for the flame-ionized detection and a Restek ShinCarbon ST Micropacked column for thermal conductivity detection.

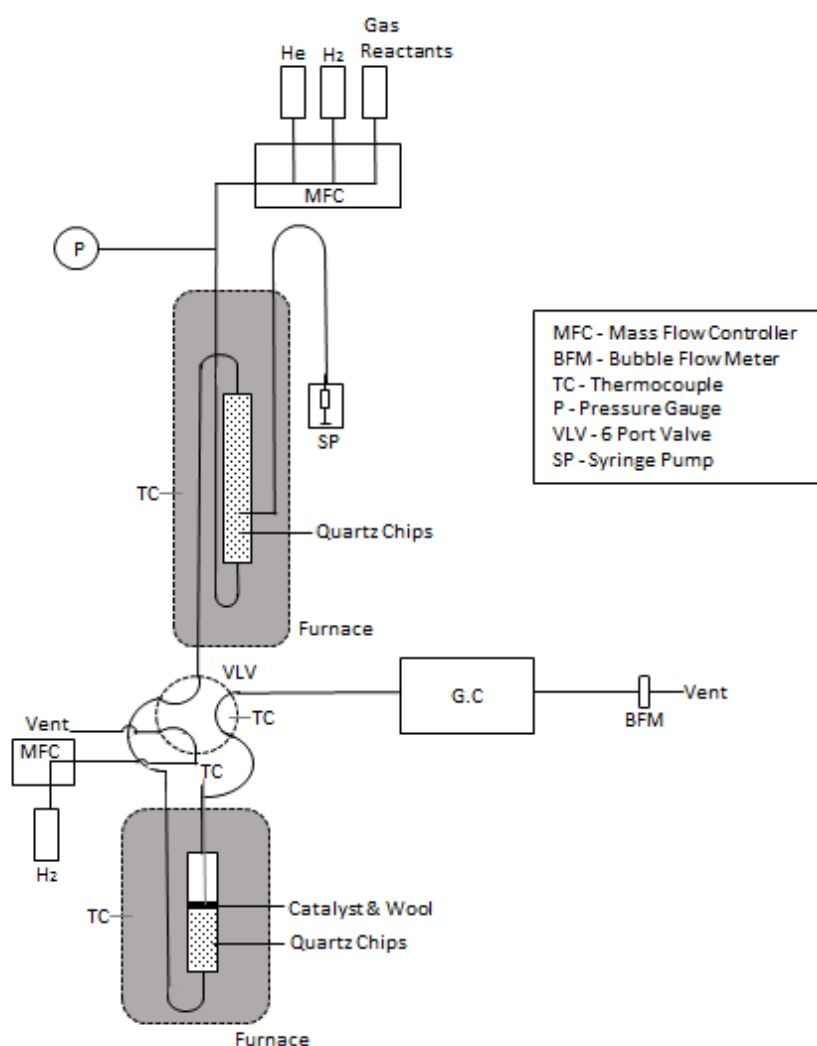


**Figure 5:** Experimental reactor setup

Carbon atom balances were performed at each reaction condition to make sure that all species were accounted for towards atom conservation; data points reported consisted of the average of multiples ones that exhibited a carbon balance of 95% or greater.

## 3.2 Results and Discussion

### 3.2.1 Tin Adsorption and Relation to pH

#### Platinum Leaching

The leaching of Pt into synthesis solution was observed in preliminary Sn adsorption and quantified using the AAS method in section 2.1.4. Upon an initial Sn adsorption experiment, it was found that over 30% of Pt had been lost from the base catalyst. It is believed that leaching occurred due to residual Pt species on the surface of the catalysts that were soluble under the acidic conditions used in the adsorption experiment. Literature has shown that PtOx surface species are dependent on the temperature at which the metal is oxidized[18]. It was hypothesized that in order to prevent Pt leaching, an additional calcination step was required to oxidize Pt species after reduction in hydrogen. Upon a second calcination step at 623 K, leaching was reduced from 30% to under 10% under the same synthesis conditions on the same batch of Pt/Al<sub>2</sub>O<sub>3</sub> seen in Table 4. This led to the addition of a calcination step after reducing and passivating catalysts in the preparation of Pt/Al<sub>2</sub>O<sub>3</sub> catalysts to be used as supports for future Sn adsorption experiments. With the addition of this step it can be assumed that Pt leaching should

**Table 4:** Platinum leaching in initial Sn adsorption experiments quantified by AAS

| Solution   | Initial pH | Final pH | Pt Lost ( $\mu\text{g}$ ) | %Pt Lost from Pt Catalyst |
|--|------------|----------|---------------------------|---------------------------|
| 200 $\mu\text{g}/\text{mL}$ Sn in HCl            | 1.05       | 1.06     | 2315                      | 33.4                      |
| 200 $\mu\text{g}/\text{mL}$ Sn in HCl (calcined) | 1.00       | 1.01     | 485                       | 7.2                       |

not be at level that will significantly impact the normalization of Sn cation uptake in the adsorption study discussed in the next section.

### Sn Uptake and Chemical Adsorption

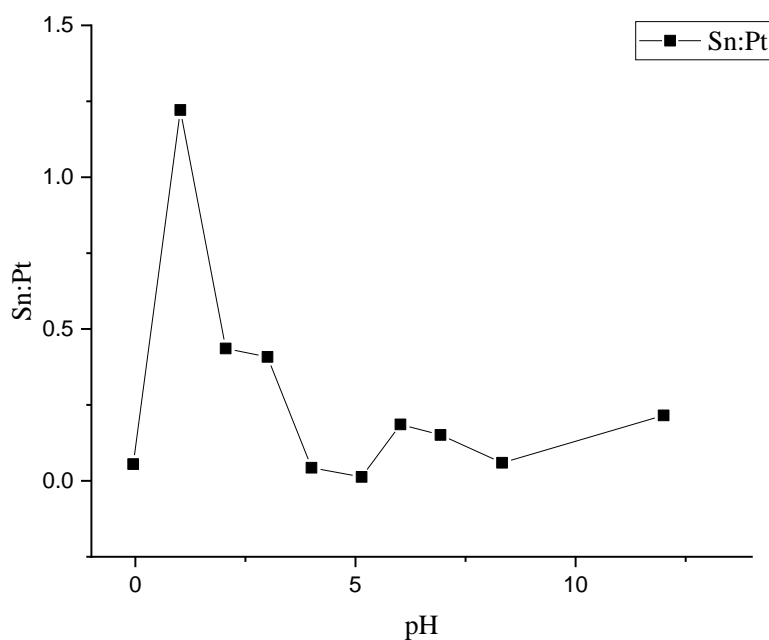


**Figure 6:** Sn adsorption normalized by the amount of Pt on the base catalyst surface over a range of synthesis pH's. Significant Sn uptake can be seen in the range of pH 1 – 3.

Given that SEA is a process dependent on pH of solution, it was necessary to conduct adsorption studies over a wide range of pH conditions. A series of Pt/Al<sub>2</sub>O<sub>3</sub> catalysts were synthesized by SEA to serve as base catalysts for Sn adsorption experiments. The ratio of base catalyst mass to synthesis solution was maintained at 4 g/L to ensure that the buffering effects of the alumina support and Pt nanoparticles remained comparable throughout the experiments. Synthesis solutions were adjusted to an initial pH from 0 to 12 and the metal loadings were determined by aqua regia digestion. As discussed earlier, the PZC of PtOx is at a pH of 1 and it was hypothesized that selective Sn adsorption to PtOx nanoparticles would occur at pH's between 1 and 4 [15]. In this range, the net charge of PtOx should be sufficiently negative while



the charge of the alumina support remained positive and would not adsorb appreciable amounts of Sn. To compare the uptake of Sn metal complexes over the experimental range, the mass of Sn adsorbed was normalized by the mass of Pt on the base catalyst used for the bimetallic synthesis. Figure 5 shows that significant Sn adsorption occurred in range of pH 1 – 3 and that some Sn appeared to be adsorbed in neutral to basic conditions. As NaOH was added to synthesis solutions, tin oxide species began precipitating out of solution and it is likely that the adsorption observed in the neutral and basic ranges is due to the presence of this particulate after filtration of the catalyst from solution. Due to the formation of solid Sn precipitates when adding NaOH, it was necessary to add only the required amount to reach the desired synthesis solutions to prevent significant loss of Sn in solution available for adsorption. This limitation prevented the pH of the synthesis solution from being controlled after the synthesis had started, therefore only the initial pH values were controlled. Table 5 shows the metal loadings of Pt and Sn determined by aqua regia digestion and ICP-MS analysis as well as the leaching of Pt during bimetallic synthesis. Observed leaching was determined insignificant in conditions of pH 1 – 12 and within the error of the digestion method. Significant leaching was seen at pH 0 and is likely due to the highly acidic synthesis conditions.

To gain a clearer picture of selective Sn adsorption it is necessary to observe the effects Sn has on the chemical adsorption of CO, H<sub>2</sub>, and O<sub>2</sub> gases on the surface of the catalyst. CO and H<sub>2</sub> will chemically adsorb to Pt at 308 K but will not chemically adsorb to Sn[14,19]. This is not the case for O<sub>2</sub>, which will adsorb to both Pt and Sn nanoparticles and therefore may be used to detect the presence of Sn on the surface when CO and H<sub>2</sub> adsorption has been suppressed from the quantities observed on Pt base catalysts[14,19]. Table 5 shows the changes in gas adsorptions and active metal dispersions with respect to the addition of Sn onto the catalyst surface. The

mass of Pt in the base catalyst was compared with the mass of Pt recovered after Sn adsorption experiments to monitor the amount of Pt leached during synthesis. All Pt-Sn catalysts had a Pt recovery within 10% when compared to the original base catalysts, which is within the error of

**Table 5:** Metal loadings of Pt/Al<sub>2</sub>O<sub>3</sub> and Pt-Sn/Al<sub>2</sub>O<sub>3</sub> catalysts. Pt-Sn/Al<sub>2</sub>O<sub>3</sub> catalysts are named for the initial pH of synthesis solution and the percent of Pt recovered from the base catalyst is provided to indicate when leaching has occurred during synthesis

| Catalyst                            | Base Catalyst                       | Pt weight (%) /<br>Sn weight (%) | Pt Recovered (%) |
|-------------------------------------|-------------------------------------|----------------------------------|------------------|
| Pt/Al <sub>2</sub> O <sub>3</sub> 1 | -                                   | 3.39 / -                         | -                |
| Pt/Al <sub>2</sub> O <sub>3</sub> 2 | -                                   | 3.38 / -                         | -                |
| Pt/Al <sub>2</sub> O <sub>3</sub> 3 | -                                   | 2.34 / -                         | -                |
| Pt/Al <sub>2</sub> O <sub>3</sub> 4 | -                                   | 2.76 / -                         | -                |
| -0.05                               | Pt/Al <sub>2</sub> O <sub>3</sub> 1 | 1.67 / 0.09                      | 49               |
| 1.02                                | Pt/Al <sub>2</sub> O <sub>3</sub> 4 | 2.49 / 3.04                      | 90               |
| 2.05                                | Pt/Al <sub>2</sub> O <sub>3</sub> 2 | 3.36 / 1.46                      | 100              |
| 3.00                                | Pt/Al <sub>2</sub> O <sub>3</sub> 4 | 3.04 / 1.24                      | 110              |
| 4.00                                | Pt/Al <sub>2</sub> O <sub>3</sub> 4 | 2.73 / 0.12                      | 99               |
| 5.14                                | Pt/Al <sub>2</sub> O <sub>3</sub> 3 | 2.47 / 0.03                      | 106              |
| 6.02                                | Pt/Al <sub>2</sub> O <sub>3</sub> 3 | 2.30 / 0.43                      | 99               |
| 6.93                                | Pt/Al <sub>2</sub> O <sub>3</sub> 4 | 2.55 / 0.39                      | 93               |
| 8.33                                | Pt/Al <sub>2</sub> O <sub>3</sub> 4 | 2.65 / 0.16                      | 96               |
| 12.00                               | Pt/Al <sub>2</sub> O <sub>3</sub> 3 | 2.37 / 0.51                      | 102              |

**Table 6:** Chemical adsorptions of CO, H<sub>2</sub>, and O<sub>2</sub> on Pt/Al<sub>2</sub>O<sub>3</sub> base catalysts and Pt-Sn/Al<sub>2</sub>O<sub>3</sub> bimetallic catalysts. Metal dispersion was calculated using CO adsorption data.

| Catalyst                            | Base Catalyst                       | CO Adsorption (μmol/g <sub>cat</sub> ) | H <sub>2</sub> Adsorption (μmol/g <sub>cat</sub> ) | O <sub>2</sub> Adsorption (μmol/g <sub>cat</sub> ) | Metal Dispersion (%) |
|-------------------------------------|-------------------------------------|--|--|--|----------------------|
| Pt/Al <sub>2</sub> O <sub>3</sub> 1 | -                                   | 149.8 ± 0.3                            | 51.0 ± 0.2   | 70.6 ± 0.5   | 86.2                 |
| Pt/Al <sub>2</sub> O <sub>3</sub> 2 | -                                   | 128.4 ± 0.2                            | 51.6 ± 0.2   | 75.7 ± 0.5   | 74.1                 |
| Pt/Al <sub>2</sub> O <sub>3</sub> 3 | -                                   | 96.0 ± 0.3                             | 34.8 ± 0.2   | 55.1 ± 0.5   | 80.0                 |
| Pt/Al <sub>2</sub> O <sub>3</sub> 4 | -                                   | 107.4 ± 0.2                            | 42.4 ± 0.3   | 59.3 ± 0.4   | 76.0                 |
| -0.05                               | Pt/Al <sub>2</sub> O <sub>3</sub> 1 | 66.3 ± 0.2                             | 20.4 ± 0.1   | 39.1 ± 0.2   | 77.4                 |
| 1.02                                | Pt/Al <sub>2</sub> O <sub>3</sub> 4 | 53.1 ± 0.4                             | 8.0 ± 0.3  | 94.6 ± 0.7   | 41.6                 |
| 2.05                                | Pt/Al <sub>2</sub> O <sub>3</sub> 2 | 101.9 ± 0.3                            | 44.5 ± 0.2   | 72.2 ± 0.6   | 59.2                 |
| 3.00                                | Pt/Al <sub>2</sub> O <sub>3</sub> 4 | 83.0 ± 0.4                             | 29.0 ± 0.3   | 67.2 ± 0.4   | 53.3                 |
| 4.00                                | Pt/Al <sub>2</sub> O <sub>3</sub> 4 | 98.1 ± 0.4                             | 36.6 ± 0.2   | 60.1 ± 0.5   | 70.1                 |
| 5.14                                | Pt/Al <sub>2</sub> O <sub>3</sub> 3 | 90.1 ± 0.2                             | 35.1 ± 0.3   | 51.3 ± 0.4   | 71.2                 |
| 6.02                                | Pt/Al <sub>2</sub> O <sub>3</sub> 3 | 83.5 ± 0.4                             | 29.1 ± 0.1   | 57.2 ± 0.5   | 70.8                 |
| 6.93                                | Pt/Al <sub>2</sub> O <sub>3</sub> 4 | 94.4 ± 0.7                             | 33.0 ± 0.3   | 54.9 ± 0.5   | 72.2                 |
| 8.33                                | Pt/Al <sub>2</sub> O <sub>3</sub> 4 | 95.4 ± 0.3                             | 36.7 ± 0.2   | 56.7 ± 0.5   | 70.2                 |
| 12.00                               | Pt/Al <sub>2</sub> O <sub>3</sub> 3 | 79.8 ± 0.2                             | 27.5 ± 0.2   | 68.9 ± 0.5   | 65.7                 |

the digestion method. Only the Pt-Sn catalyst synthesized at pH 0 had significant Pt loss which is likely due to the highly acidic environment during Sn adsorption.

The percent metal dispersion of active metals was calculated using the quantities obtained from CO adsorption and is defined as:

$$\%M_{\text{DISP}} = \frac{100\% \times 100\%}{22414} \times \frac{V \times SF}{\frac{\% \text{weight Pt}}{W_{\text{Pt}}}}$$

where  $V$  ( $\text{cm}^3/\text{g}$  STP) is the quantity of gas chemically adsorbed to the surface,  $SF_{\text{CALC}}$  is the calculated stoichiometry factor (1 for CO), %weight Pt is the weight percent of Pt in the sample,  $W_{\text{Pt}}$  is the atomic weight of Pt (195.090 g/mol), and 22414 ( $\text{cm}^3$  STP/mole of gas) is the volume occupied by one mole of gas. CO adsorption data shows very high metal dispersions, 75 – 85%, in base Pt catalysts, which is indicative of the small nanoparticle sizes predicted by the SEA method. In conditions where little to no Sn is expected to adsorb to PtOx surface species, it was found that the amount of Pt that was available for CO adsorption remained above 70%, remaining comparable to the base catalysts used for synthesis. This change can be attributed to the multiple calcination and reduction cycles that Pt nanoparticles underwent from base catalyst and bimetallic catalyst synthesis, as shown in Table 6, where multiple chemisorption experiments on the same Pt monometallic catalyst displayed an initial decrease in metal dispersion before reaching a stable surface environment. CO and H<sub>2</sub> adsorptions were suppressed at synthesis pH's 1 – 3 when compared to the adsorptions on base catalysts, which corresponds with the Sn uptakes observed in Figure 5 and confirms that there is some degree of Pt-Sn interaction on the surface.

**Table 7:** Pt/Al<sub>2</sub>O<sub>3</sub> 1 CO adsorption results showing initial drops in metal dispersion with multiple reductions.

| Trial | CO Adsorption ( $\mu\text{mol/g}_{\text{cat}}$ ) | Metal Dispersion (%) |
|-------|--|----------------------|
| 1     | 149.8 $\pm$ 0.3                                  | 86.2                 |
| 2     | 126.1 $\pm$ 0.3                                  | 72.6                 |
| 3     | 120.7 $\pm$ 0.6                                  | 69.5                 |
| 4     | 117.4 $\pm$ 0.3                                  | 67.5                 |
| 5     | 115.9 $\pm$ 0.4                                  | 66.7                 |

### Electron Microprobe X-ray Mapping

Electron microprobe experiment were conducted on a 2.56wt%/2.53wt% Pt-Sn/Al<sub>2</sub>O<sub>3</sub> catalyst synthesized at a pH of 1 to collect Pt L $\alpha$  and Sn L $\alpha$  x-ray data and construct a surface map of Pt and Sn regions seen in Figure 6. While the resolution of the microprobe is not sufficient enough to scan individual nanoparticles, it does confirm Sn adsorption to the surface of the Pt/Al<sub>2</sub>O<sub>3</sub> base catalyst. In order to determine the extent of selective Sn adsorption to Pt nanoparticles, it would be necessary to conduct a similar experiment using transmission electron microscopy (TEM), which would be capable of resolving individual nanoparticles on the surface of the catalyst. It is worth noting that there appears to be a correlation between regions with significant Sn L $\alpha$  x-ray response and those with higher Pt L $\alpha$  response.

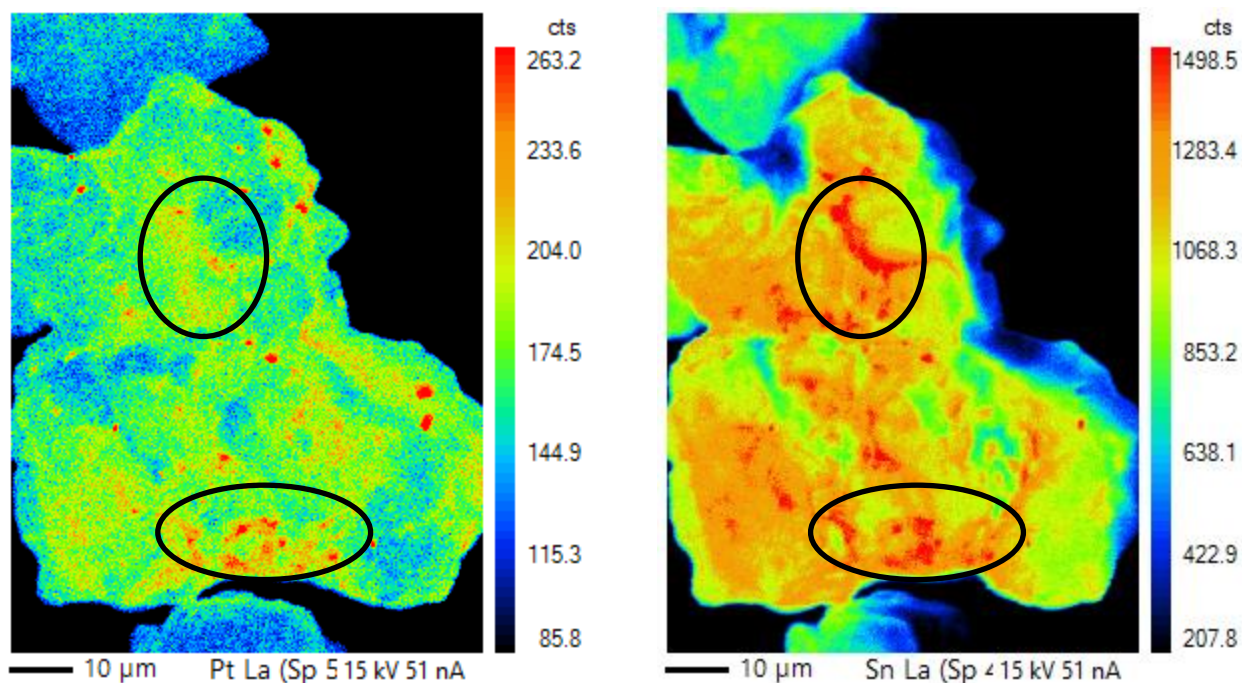


**Figure 7:** Pt  $L\alpha$  (left) and Sn  $L\alpha$  (right) x-ray mapping of a 2.56%Pt/2.53%Sn bimetallic catalyst. Circled areas indicate regions of possible corresponding Pt and Sn intensities.

### 3.2.2 Effects of Tin on Platinum Catalysts

Though chemisorption and metal loading experiments are capable of showing the adsorption of Sn and the possibility of Pt-Sn interactions, it was necessary to conduct more detailed characterizations of the effects Sn has on Pt active sites. This section will discuss the use of different characterization techniques, along with probe reaction experiments conducted in a packed bed reactor (PBR) aimed at testing the performance of bimetallic catalysts in a practical setting. The use of these techniques should provide insights on the changes in reaction chemistry when Sn is present on the surface.

#### Reactor Performance

Pt/ $\text{Al}_2\text{O}_3$  and Pt-Sn/ $\text{Al}_2\text{O}_3$  catalysts were loaded into a packed bed reactor (PBR) and used to for propionic acid hydrodeoxygenation (HDO). The desired products of this reaction are the partially oxygenated species, propanol and propionaldehyde. Figure 7 is a comparison of the

products formed during propionic acid HDO over monometallic and bimetallic catalysts. There was a higher product diversity over Pt/Al<sub>2</sub>O<sub>3</sub> compared to Pt-Sn/Al<sub>2</sub>O<sub>3</sub> at comparable conversions which is indicative of undesired chemistries occurring over the monometallic surface. The products of these undesired pathways include carbon monoxide, carbon dioxide, methane, ethane, and propane. It is observed that the addition of Sn drastically changes the selectivity of propionic acid HDO products as the undesired pathways were suppressed while the selectivity of the partially oxygenated species increased. This provides useful insight into the potential impact of bimetallic catalysts in the area of catalysts used in the industrial production of chemicals. Further characterization of Pt-Sn/Al<sub>2</sub>O<sub>3</sub> catalysts would shed light on the interaction(s) between Pt and Sn nanoparticles on the catalyst surface, which can further elucidate the reason for the better product selectivity over bimetallic catalysts.

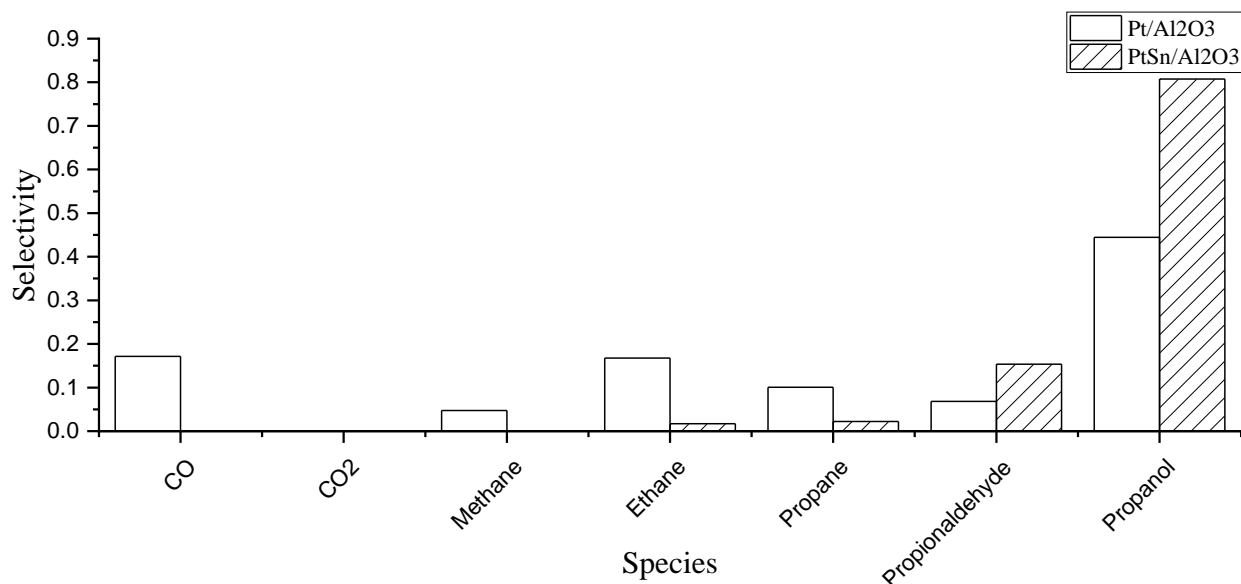


**Figure 8:** Changes in selectivity of HDO, methanation, hydrogenolysis, and water-gas shift reactions at 469 K, 5 torr propionic acid, and 755 torr H<sub>2</sub>.

### Temperature Programmed Reduction (TPR)

Temperature programmed reductions (TPR) provide information regarding the reducibility of surface metals and may be able to be linked to the changes observed in reaction chemistry. For instance, PtOx species may be prevented from reducing to a completely metallic state due to the oxophilic properties of Sn present on the surface[12]. This change in the reduced state of PtOx may alter the adsorptive properties of active sites and provide an answer to the changes in propionic acid HDO selectivities seen in the previous section. Figure 8 shows the reduction profiles of the alumina support, three catalysts synthesized using the commonly used method of incipient wetness impregnation (IW), and two catalysts synthesized using the SEA method. The metal loading of these catalysts is summarized in Table 7.

**Table 8:** Metal loadings of SEA and IW catalysts used in TPR experiments

| Catalyst  | Pt Weight (%) / Sn Weight (%) |
|-----------|-------------------------------|
| SEA Pt/Sn | 2.49 / 3.04                   |
| SEA Pt    | 2.69 / -                      |
| IW Pt/Sn  | 3.33 / 1.22                   |
| IW Sn     | - / 4.08                      |
| IW Pt     | 3.37 / -                      |

Catalysts containing Pt all show two H<sub>2</sub> uptake peaks in the 350 – 450 K range. These peaks can be attributed to the reduction of two separate Pt oxidation states. For instance, the initial consumption of H<sub>2</sub> may be reducing Pt<sup>4+</sup> species to Pt<sup>2+</sup> followed by a second H<sub>2</sub> consumption peak where Pt is being reduced to a metallic state[20–22]. The third reduction peak shown for Pt samples, 650 – 750 K, may be attributed to the partial reduction of the alumina support where it is in contact with Pt nanoparticles[12]. For completeness, TPR analysis was



conducted on a Sn IW catalyst which shows no appreciable H<sub>2</sub> uptake within the temperature ranges of the experiment. This can be attributed to the extreme temperatures needed to reduce Sn when it is the only metal on the catalyst surface[23]. Both the SEA and IW Pt-Sn catalysts show an increase in the second reduction peak which may indicate that Pt species are in a higher oxidation state and therefore require higher temperatures for complete reduction. The increased H<sub>2</sub> consumption 650 – 750 K is possibly due to Sn being reduced to a metallic state as other works have shown that it possible to reduce Sn at lower temperatures when it is proximity of metal capable of hydrogen dissociation at lower temperatures[12,23]. The SEA bimetallic shows a third reduction peak within the realm of initial platinum reduction, which may be attributed to H<sub>2</sub> spilling, indicating the possible alloying Pt and Sn nanoparticles[12,20]. This third peak may also imply that a third oxidation state of Pt is present and requires higher temperatures to be reached before reducing to a metallic state. This would imply that changes in propionic acid

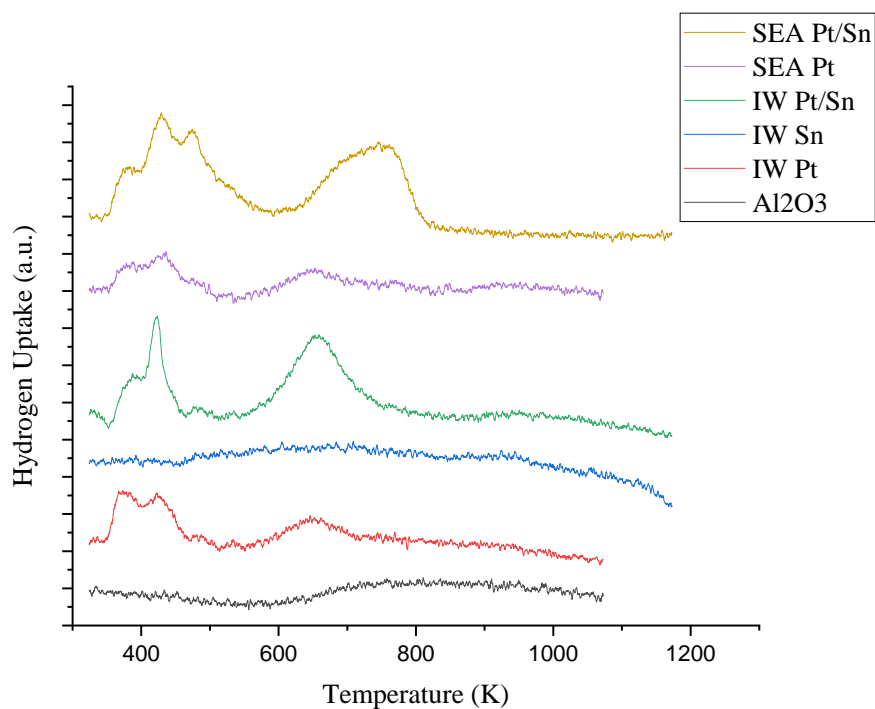


**Figure 9:** TPR profiles of mono and bimetallic catalysts synthesized using IW and SEA methods.

HDO selectivities may be attributed to Pt species remain partially oxidized under reaction conditions, therefore altering the adsorptive properties of active sites on Pt-Sn/Al<sub>2</sub>O<sub>3</sub> catalysts.

### Ambient Pressure Photoemission Spectroscopy

Ambient pressure photoemission spectroscopy (AP-PES) data was collected on three catalysts, metal loadings summarized in Table 8, in 1 mbar H<sub>2</sub> at 575 K to simulate reaction conditions after the catalysts has been reduced to its active state. Scans were focused on the Al2p and Pt4f lines and referenced to the position of the maximum intensity of the Al2s line to account for charging effects and interference from the electronic current passing through the heating element under the sample holder. All scans were found to have a difference of  $44.7 \pm 0.4$  eV in binding energy between the maximum Al2s line and maximum Al2p line suggesting that the changes in Pt oxidation states are real. AP-PES scans were deconvoluted using KolXP software. The spectra of the Pt/Al<sub>2</sub>O<sub>3</sub> catalyst, Figure 9a, shows a large response at the Al2p line with a smaller shoulder at the Pt4f line. The same is seen in the fresh PtSn/Al<sub>2</sub>O<sub>3</sub> catalyst, Figure 9b, but with a greater shoulder due to a shift in binding energy at the Pt4f line. The spent PtSn/Al<sub>2</sub>O<sub>3</sub> spectra, Figure 9c, has two shoulders at the Pt4f line, indicating that some surface change has occurred while in the reactor during probe reactions, causing Pt to be in two separate oxidation states on the surface[20,24,25].

**Table 9:** Metal loadings of SEA catalysts used in AP-PES experiments

| Catalyst                                   | Pt Weight (%) / Sn Weight (%) |
|--|-------------------------------|
| Pt/Al <sub>2</sub> O <sub>3</sub>          | 3.39 / -                      |
| Fresh Pt-Sn/Al <sub>2</sub> O <sub>3</sub> | 2.56 / 2.53                   |
| Spent Pt-Sn/Al <sub>2</sub> O <sub>3</sub> | 2.56 / 2.53                   |

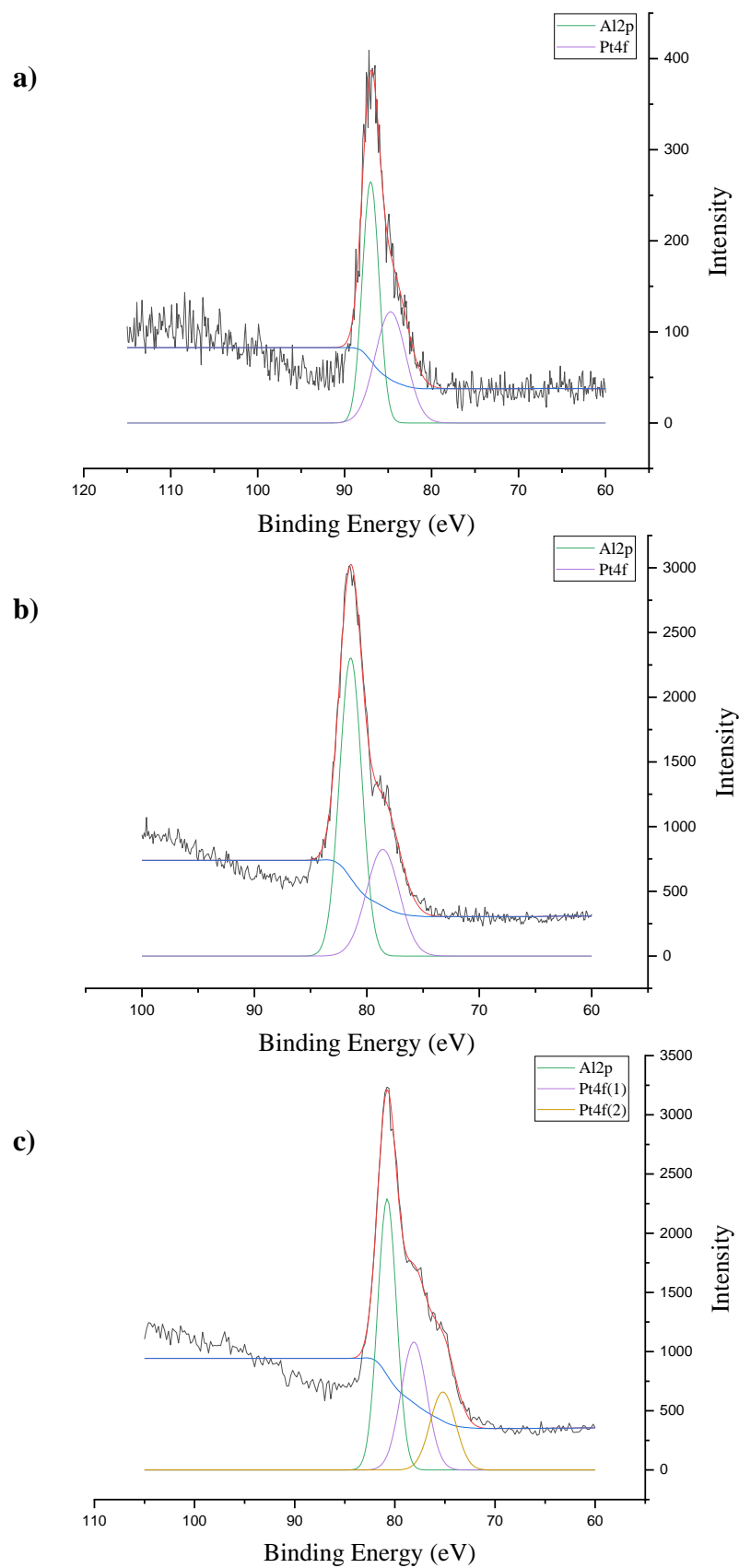


**Figure 10:** a) Al<sub>2</sub>p and Pt<sub>4</sub>f lines of a Pt/Al<sub>2</sub>O<sub>3</sub> catalyst b) Al<sub>2</sub>p and Pt<sub>4</sub>f lines of a fresh Pt-Sn/Al<sub>2</sub>O<sub>3</sub> catalyst c) Al<sub>2</sub>p and Pt<sub>4</sub>f lines of a spent Pt-Sn/Al<sub>2</sub>O<sub>3</sub> catalyst

Similar to the TPR experiments discussed in the previous section, the presence of multiple Pt oxidation states in AP-PES spectra may imply that changes in propionic acid HDO selectivities are attributed to Pt species remaining partially oxidized under reaction conditions.

### **3.3 Conclusion**

It is clear that the SEA method of catalyst synthesis is useful in the adsorption of Sn over Pt/Al<sub>2</sub>O<sub>3</sub> base catalysts as shown by metal loadings and confirmed by electron microprobe analysis. Sn adsorption was seen across a wide range of both acidic and basic conditions, with the observed maximum uptake between pH's 1 and 3. Pt-Sn/Al<sub>2</sub>O<sub>3</sub> catalysts exhibit reduced chemical adsorption of CO and H<sub>2</sub> gases, which suggests that Sn addition has caused a geometric and/or an electronic change to the base monometallic surface, and is reflected in the shifts in selectivity observed in propionic acid HDO experiments. TPR and AP-PES data suggest that Pt metal sites are present in multiple oxidation states under reaction conditions, providing a plausible explanation for the shifts in selectivities.

## **Chapter 4. Conclusion**

### **4.1 Current Work**

This work has shown that SEA method is a simple and useful tool for the controlled synthesis of Pt-Sn bimetallic catalysts that have profound effects on the selectivity of propionic acid HDO. These catalysts are capable of suppressing the unwanted pathways of methanation, hydrogenolysis, and decarbonylation, allowing for almost 100% of selectivity to be shifted toward desired products. Through AP-PES and TPR experiments, this work has shown it is likely that Sn is perturbing the oxidation state of Pt active sites under reaction conditions, thus enabling the observed shifts in reaction selectivity.

This work has shown promise in the ability to tune catalysts to be selective toward propionic acid HDO products and provides a useful first step in their application in targeting specific functional groups in the upgrading of biomass sourced succinic acid. A number of groups have shown significantly improved selectivity of succinic acid HDO products in bimetallic systems: Ru-Sn/PAC (powder active carbon), Pt-Sn/PAC, Ir-Re/C, Pd-Re/TiO<sub>2</sub>, Pd-Cu/AX (alumina xerogel), Pd-Re/C, and Ru-Re/C[4,19,26–28]. The results of these studies lend promise to the observed changes in propionic acid HDO selectivities directly translating to succinic acid feedstocks.

### **4.2 Future Work**

While current work proves SEA to be a viable method for synthesizing Pt-Sn bimetallic supported catalysts, further characterization is still necessary to provide a clearer picture as to the extent of selective Sn adsorption at the observed optimal synthesis conditions.

Transmission electron microscopy (TEM) coupled with energy-dispersive x-ray spectroscopy (EDXS) would provide greater insight into the extent of selective adsorption and

confirm the particle size and tight distribution hypothesized by the method. EDXS would also provide information on the structure of bimetallic nanoparticles (core-shell or mixed alloy) and the homogeneity of surface species. Higher resolution XRD analysis would also be a useful tool to circumvent the issue of alumina background signal in the bulk catalyst powder. This analysis would allow for the identification of Pt, Sn, and Pt-Sn species on the surface of the catalyst, as well as identify the presence of any bulk Sn precipitate that was formed during synthesis at pH's requiring the addition of NaOH to reach targeted conditions.

Further experimentation with the controlled synthesis of Pt-Sn nanoparticles may provide more insight into the tuning of catalysts for HDO selectivity. With information on the optimal synthesis conditions for selective secondary metal adsorption, it may be possible to control catalyst synthesis to obtain more exact metal loading ratios through multiple adsorptions to optimize reactor performance.

## References

- [1] T.W. Walker, A.H. Motagamwala, J.A. Dumesic, G.W. Huber, Fundamental catalytic challenges to design improved biomass conversion technologies, *J. Catal.* (2018). doi:10.1016/j.jcat.2018.11.028.
- [2] D.M. Alonso, S.G. Wettstein, J.A. Dumesic, Bimetallic catalysts for upgrading of biomass to fuels and chemicals, *Chem. Soc. Rev.* 41 (2012) 8075–8098. doi:10.1039/c2cs35188a.
- [3] J. Regalbuto, An NSF perspective on next generation hydrocarbon biorefineries, *Comput. Chem. Eng.* 34 (2010) 1393–1396. doi:10.1016/j.compchemeng.2010.02.025.
- [4] J.M. Keels, X. Chen, S. Karakalos, C. Liang, J.R. Monnier, J.R. Regalbuto, Aqueous-Phase Hydrogenation of Succinic Acid Using Bimetallic Ir-Re/C Catalysts Prepared by Strong Electrostatic Adsorption, *ACS Catal.* 8 (2018) 6486–6494. doi:10.1021/acscatal.8b01006.
- [5] A. Chatzidimitriou, J.Q. Bond, Oxidation of levulinic acid for the production of maleic anhydride: breathing new life into biochemicals, *Green Chem.* 17 (2015) 4367–4376. doi:10.1039/c5gc01000d.
- [6] D.M. Alonso, S.G. Wettstein, J.A. Dumesic, Gamma-valerolactone, a sustainable platform molecule derived from lignocellulosic biomass, *Green Chem.* 15 (2013) 584–595. doi:10.1039/c3gc37065h.
- [7] T. Werpy, G. Petersen, *Top Value Added Chemicals from Biomass: Volume 1 — Results of Screening for Potential Candidates from Sugars and Synthesis Gas*, 2004. doi:10.2172/15008859.
- [8] D. Cimini, L. Zaccariello, S. D’Ambrosio, L. Lama, G. Ruoppolo, O. Pepe, V. Faraco, C. Schiraldi, Improved production of succinic acid from *Basfia succiniciproducens* growing on A. donax and process evaluation through material flow analysis, *Biotechnol. Biofuels.* 12 (2019) 1–14. doi:10.1186/s13068-019-1362-6.
- [9] K.-K. Cheng, X.-B. Zhao, J. Zeng, R.-C. Wu, Y.-Z. Xu, D.-H. Liu, J.-A. Zhang, Downstream processing of biotechnological produced succinic acid, *Appl. Microbiol. Biotechnol.* 95 (2012) 841–850. doi:10.1007/s00253-012-4214-x.
- [10] K.-K. Cheng, X.-B. Zhao, J. Zeng, J.-A. Zhang, Biotechnological production of succinic acid: current state and perspectives, *Biofuels, Bioprod. Bioref.* 6 (2012) 302–318. doi:10.1002/bbb.
- [11] Y. Elkasabi, Q. Liu, Y.S. Choi, G. Strahan, A.A. Boateng, J.R. Regalbuto, Bio-oil hydrodeoxygenation catalysts produced using strong electrostatic adsorption, *Fuel.* 207 (2017) 510–521. doi:10.1016/j.fuel.2017.06.115.
- [12] K.A. Resende, C.A. Teles, G. Jacobs, B.H. Davis, D.C. Cronauer, A. Jeremy Kropf, C.L. Marshall, C.E. Hori, F.B. Noronha, Hydrodeoxygenation of phenol over zirconia supported Pd bimetallic catalysts. The effect of second metal on catalyst performance, *Appl. Catal. B Environ.* 232 (2018) 213–231. doi:10.1016/j.apcatb.2018.03.041.
- [13] A. Wong, Q. Liu, S. Griffin, A. Nicholls, J.R. Regalbuto, Synthesis of ultrasmall, homogeneously alloyed, bimetallic nanoparticles on silica supports, *Science* (80-. ). 358 (2017) 1427–1430. doi:10.1126/science.aao6538.
- [14] S.G. Wettstein, J.Q. Bond, D.M. Alonso, H.N. Pham, A.K. Datye, J.A. Dumesic, RuSn bimetallic catalysts for selective hydrogenation of levulinic acid to  $\gamma$ -valerolactone, *Appl. Catal. B Environ.* 117–118 (2012) 321–329. doi:10.1016/j.apcatb.2012.01.033.

- [15] H.-R. Cho, J.R. Regalbuto, The rational synthesis of Pt-Pd bimetallic catalysts by electrostatic adsorption, *Catal. Today*. 246 (2015) 143–153. <http://scholarcommons.sc.edu/etd/2484>.
- [16] L. Jiao, J.R. Regalbuto, The synthesis of highly dispersed noble and base metals on silica via strong electrostatic adsorption: I. Amorphous silica, *J. Catal.* 260 (2008) 329–341. doi:10.1016/j.jcat.2008.09.022.
- [17] Manipulator heater module for NAP conditions, SPECS Surface Nano Analysis GmbH, n.d.
- [18] C.-P. Hwang, C.-T. Yeh, Platinum-oxide species formed by oxidation of platinum crystallites supported on alumina, *J. Mol. Catal. A Chem.* 112 (1996) 295–302. doi:10.1016/1381-1169(96)00127-6.
- [19] D.R. Vardon, A.E. Settle, V. Vorotnikov, M.J. Menart, T.R. Eaton, K.A. Unocic, K.X. Sterirer, K.N. Wood, N.S. Cleveland, K.E. Moyer, W.E. Michener, G.T. Beckham, Ru-Sn/AC for the Aqueous-Phase Reduction of Succinic Acid to 1,4-Butanediol under Continuous Process Conditions, *ACS Catal.* 7 (2017) 6207–6219. doi:10.1021/acscatal.7b02015.
- [20] D.L. Hoang, S.A.-F. Farrage, J. Radnik, M.-M. Pohl, M. Schneider, H. Lieske, A. Martin, A comparative study of zirconia and alumina supported Pt and Pt–Sn catalysts used for dehydrocyclization of n-octane, *Appl. Catal. A Gen.* 333 (2007) 67–77. doi:10.1016/j.apcata.2007.09.003.
- [21] J. Salmones, J.-A. Wang, J.A. Galicia, G. Aguilar-Rios, H<sub>2</sub> reduction behaviors and catalytic performance of bimetallic tin-modified platinum catalysts for propane dehydrogenation, *J. Mol. Catal. A Chem.* 184 (2002) 203–213. doi:10.1016/S1381-1169(01)00525-8.
- [22] A.S. Ivanova, E.M. Slavinskaya, R. V. Gulyaev, V.I. Zaikovskii, O.A. Stonkus, I.G. Danilova, L.M. Plyasova, I.A. Polukhina, A.I. Boronin, Metal-support interactions in Pt/Al<sub>2</sub>O<sub>3</sub> and Pd/Al<sub>2</sub>O<sub>3</sub> catalysts for CO oxidation, *Appl. Catal. B Environ.* 97 (2010) 57–71. doi:10.1016/j.apcatb.2010.03.024.
- [23] R. Sasikala, S.K. Kulshreshtha, Temperature programmed reduction studies of spillover effect in Pd impregnated metal oxide catalysts, *J. Therm. Anal. Calorim.* 78 (2004) 723–729. doi:10.1007/s10973-005-0438-0.
- [24] A.S. Karakoti, J.E.S. King, A. Vincent, S. Seal, Synthesis dependent core level binding energy shift in the oxidation state of platinum coated on ceria-titania and its effect on catalytic decomposition of methanol, *Appl. Catal. A Gen.* 388 (2010) 262–271. doi:10.1016/j.apcata.2010.08.060.
- [25] F. Şen, G. Gökağaç, Different sized platinum nanoparticles supported on carbon: An XPS study on these methanol oxidation catalysts, *J. Phys. Chem. C*. 111 (2007) 5715–5720. doi:10.1021/jp068381b.
- [26] B.K. Ly, D.P. Minh, C. Pinel, M. Besson, B. Tapin, F. Epron, C. Especel, Effect of addition mode of Re in bimetallic Pd-Re/TiO<sub>2</sub> catalysts upon the selective aqueous-phase hydrogenation of succinic acid to 1,4-butanediol, *Top. Catal.* 55 (2012) 466–473. doi:10.1007/s11244-012-9813-3.
- [27] S.C. Patankar, A.G. Sharma, G.D. Yadav, Biobased process intensification in selective synthesis of  $\gamma$ -butyrolactone from succinic acid via synergistic palladium–copper bimetallic catalyst supported on alumina xerogel, *Clean Technol. Environ. Policy*. 20 (2018) 683–693. doi:10.1007/s10098-017-1381-6.



- [28] D. Pham Minh, M. Besson, C. Pinel, P. Fuertes, C. Petitjean, Aqueous-phase hydrogenation of biomass-based succinic acid to 1,4-butanediol over supported bimetallic catalysts, *Top. Catal.* 53 (2010) 1270–1273. doi:10.1007/s11244-010-9580-y.

**Vita****Name of Author:**

Patrick Michael Howe

**Place of Birth:**

Syracuse, New York

**Date of Birth:**

April 10, 1990

**Undergraduate School Attended:**

Stony Brook University, Stony Brook, New York

**Degree Awarded:**

Bachelor of Science in Marine Vertebrate Biology, 2013, Stony Brook University  
Minor in Ecosystems and Human Impact